International Journal of Innovative Computing, Information and Control
Volume **18**, Number **1**, February **2022**

 ISSN 1349-4198
pp. **149–159**

IMAGE ENHANCEMENT OF ROBOT WELDING SEAM BASED ON WAVELET TRANSFORM AND CONTRAST GUIDANCE

Yiying Zhao[1] and Qingjiu Huang[2,*]

[1]School of Information and Electronic Engineering
Zhejiang Gongshang University
No. 18, Xuezheng Street, Xiasha University Town, Hangzhou 310018, P. R. China
15967148931@163.com

[2]Control System Laboratory
Graduate School of Engineering
Kogakuin University
1-24-2 Nishi-Shinjuku, Tokyo 163-8677, Japan
*Corresponding author: huang@cc.kogakuin.ac.jp

Received August 2021; revised November 2021

Abstract. *With the increasing of needs for machine vision in the field of robotic welding, how to improve the resolution of weld seam images with high fidelity has become an important research topic in machine vision. Therefore, this paper proposes an image enhancement algorithm of robot welding seam based on wavelet transform and contrast guidance. First, the weld seam image is pre-interpolated, which means that the wavelet transform algorithm is introduced in the process of enhancing the image resolution in advance, so that the high-frequency information of the weld seam part, which means the collection of edge points of the image will not be lost during the interpolation process. Then, we use contrast guidance to precisely position the edge points of the pre-interpolated image, and obtain the pixel values of an edge point more accurately according to the weight ratio equation of known pixels around this edge point, so as to avoid the jaggedness and blurring effect of the edge parts caused by the existing interpolation algorithms. Finally, this paper shows the effectiveness of this algorithm through experiments of image enhancement on stud welding of anchor chains using robot and based on the comparison results between this algorithm and other algorithms.*

Keywords: Robotic welding, Image enhancement, Image interpolation, Weld seam image

1. **Introduction.** With the increasing of needs for welding robots in the non-standard parts manufacturing, the technology researches and development of machine vision based intelligent welding robots are imperative. However, the technology of machine vision applied to the non-standard parts robot welding on the current market relies heavily on high-resolution camera equipment, which can increase production costs [1, 2, 3, 4]. Therefore, the use of software to improve the resolution of weld seam images by means of low-resolution camera equipment is a current research approach to machine vision. Image interpolation is a form of software that can improve the resolution of the acquired digital images without increasing the performance of the camera equipment [5].

Lots of studies on image interpolation have been done so far. Traditional algorithms in linear interpolation include the nearest field interpolation, bilinear interpolation, and bicubic interpolation [6, 7]. Although the time complexity of these existing algorithms of linear interpolation is low, the essence of the linear interpolation algorithm is similar to the

DOI: 10.24507/ijicic.18.01.149

low-pass filter, so it will weaken the high-frequency information in the original images. To improve the weakening of high-frequency information, an image interpolation algorithm based on wavelet transform and bicubic interpolation was proposed [8]. However, the linear interpolation algorithm is still used in the interpolation of high-frequency information, so the probability of noise is increased. Meanwhile, another high-performance image resolution enhancement algorithm based on wavelet-based image interpolation has been proposed [9]. However, the computational effort increases substantially because polynomial curve fitting is used to establish a linear relationship between the actual and predicted high-frequency subbands. On the other hand, an edge-guided image interpolation method using Taylor series approximation has been proposed to better preserve the information of the edge part of the image and reduce the jaggedness of the edge part [10]; although the interpolation effect of this algorithm is good, it is complicated and difficult to implement in hardware. Another algorithm applies the second-order Newton interpolation method to the image adaptive scaling process [11]; although the complexity of this algorithm is low and facilitates hardware implementation, the image sharpness is still a certain gap compared to other algorithms. Simultaneously, a contrast interpolation algorithm based on image edges was proposed, and the concept of edge diffusion was introduced [12]. However, when the algorithm interpolates more pixels from the limited original image information, it will produce errors, especially when calculating the pixels near the edge.

Considering the above, this study proposes an image enhancement algorithm for robotic welding seams based on wavelet transform and contrast guidance, which can preserve the high-frequency information in the original image to the greatest extent and accurately interpolate each edge point, thereby reducing the jaggedness of the image enhanced by the interpolation. Specifically, first, the weld image is pre-interpolated, that is, the wavelet transform algorithm is introduced in the process of pre-enhancing the image resolution, so that the high-frequency information of the weld part, which means the set of edge points of the image, will not be lost during the interpolation process. Then, the pre-interpolated image is precisely positioned at the edge points using contrast guidance, and the pixel values of the edge points are more accurately derived based on the weight ratio equation of known pixels around the edge points, so as to avoid the jaggedness and blurring effect of the edge parts brought about by existing interpolation algorithms. Finally, to verify the effectiveness of the algorithm proposed in this study, a comparison between the existing interpolation algorithm and the proposed algorithm will be preformed through the experiments of image enhancement on stud welding of anchor chains using robot as shown in Figure 1.

Applying the algorithm to the weld image pre-processing step in the anchor chain welding process achieves the same weld image accuracy accomplished by a low pixel camera as a high pixel camera, while the impact on the subsequent weld after processing is close to the same. However, the application of the algorithm saves a handful of equipment costs as well as labor costs for small and medium-sized enterprises.

2. **Existing Image Interpolation Algorithms.**

Image interpolation algorithm has always been a research hot spot in the field of image processing, which can be mainly divided into linear interpolation algorithms and nonlinear interpolation algorithms.

2.1. **Linear interpolation algorithms.**

2.1.1. *Nearest field interpolation algorithm.* The core principle of the nearest field interpolation algorithm is to take the pixel value of the neighboring point with the shortest Euclidean distance from the point to be inserted as the pixel value of the point to be

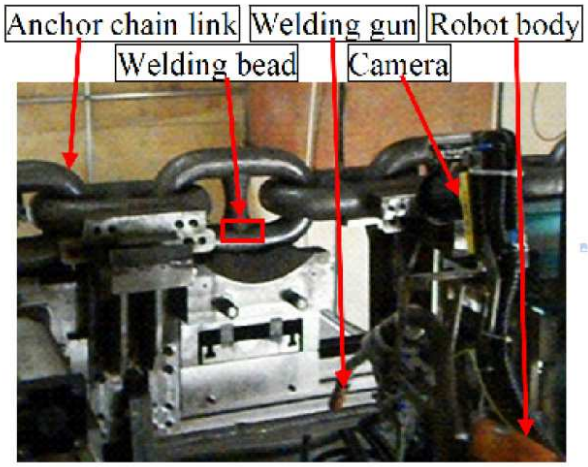

FIGURE 1. Stud welding of anchor chains

inserted. This algorithm is widely used in image enhancement processing due to the advantage of computational simplicity. However, it only considered the mode of a single neighboring point, which will cause a certain amount of image blur.

2.1.2. *Bilinear interpolation algorithm.* The interpolation principle of the bilinear interpolation algorithm is to obtain the pixel value of the point to be inserted by linearly interpolating it with its neighboring pixel points in two linear directions. This algorithm overcomes the interpolation error of the nearest field algorithm to a certain extent, but because it ignores the influence of the pixel value change rate between adjacent points, the high-frequency information of the image is damaged and the image edges are blurred.

2.1.3. *Bicubic interpolation algorithm.* The basic idea of the bicubic interpolation algorithm is to obtain the pixel value of the point to be inserted by using the third-order interpolation of 16 known pixel points centered on the point to be inserted. This algorithm considers the effect of the rate of change of pixel values between each neighboring point, so that the final obtained interpolated image has a higher resolution, but the number of pixel points to be calculated increases, making the amount of operations significantly higher than the previous two interpolation algorithms.

2.2. **Nonlinear interpolation algorithms.**

2.2.1. *Wavelet transform based interpolation algorithm.* The linear interpolation algorithm is a direct processing of pixel values on the spatial domain, which causes some loss of high-frequency information on the image edges. The wavelet transform based interpolation algorithm transforms the process of image interpolation into the frequency domain, and separates the high- and low-frequency information of the image, so that the high-frequency information can be processed separately; thus, it compensates the disadvantage of serious loss of high-frequency information at the edge of the linear interpolation algorithm [13, 14, 15]. Of course, this interpolation algorithm also has limitations, for example, the high accuracy for edge detection algorithms is required and the noise is introduced in the interpolation process due to the lack of a universal standard for the selection of wavelet bases.

2.2.2. *Edge information based interpolation algorithm.* Besides wavelet transform based interpolation algorithms, a number of algorithms based on edge high-frequency information to guide image interpolation have been proposed successively [16, 17, 18]. These

algorithms improve the clarity of the edge portion of the image by targeted interpolation and amplification of the high-frequency information at the edges. Some edge based interpolation algorithms, such as CGI [12], still have the disadvantage of direction confusion of edge point interpolation when the image edge information is complex.

2.2.3. *Deep learning based interpolation algorithm.* In order to better improve the accuracy of the final image, many algorithms that apply deep learning techniques, such as deep convolutional neural networks, to image interpolation have emerged [19, 20, 21, 22]. However, these algorithms require a large amount of training data and perfect hardware conditions upfront to obtain better image accuracy, so they are not suitable for the needs of small and medium-sized enterprises.

3. **Interpolation Algorithm Based on Wavelet Transform and Contrast Guidance.** In an image, the edge region is the most critical component of the image, and is a collection of pixel points that produce leaps within the image, therefore containing a lot of useful information [13]. In response to the shortcomings of the existing interpolation algorithms described in Section 2, which are blur of edge parts, large calculations, high requirements of edge detection algorithms, and confusion of interpolation of edge points, this paper proposes an interpolation algorithm based on wavelet transform and contrast guidance. Specifically, the two-dimensional discrete wavelet transform is used to ensure that the image edge information is not lost to the maximum extent. And then, the algorithm of diffusion contrast in CGI algorithm is used to precisely position and calculate the edge points of the image, so as to avoid the jagged phenomenon and blurring effect of the edge part brought by the existing interpolation algorithm.

The operation flowchart of the interpolation algorithm based on wavelet transform and contrast guidance proposed in this paper is shown in Figure 2. Firstly, the low-resolution image (LR) is decomposed into four sub-images containing different frequency information by a two-dimensional discrete wavelet transform; Then, the sub-images containing high-frequency information are enlarged based on the linear interpolation algorithm, and the enlarged image and the original LR image are transformed by wavelet reconstruction to obtain the pre-interpolated high-resolution image (hereinafter referred to as HR); And then, the value of diffusion contrast of each pixel in the pre-interpolated HR image is calculated, and this is used to form the decision map to guide the interpolation process; Finally, in order to form the final interpolated high-resolution image, the pixel value of each edge point is calculated according to the contrast decision map as well as the weight ratio equations. The main operating steps are described as follows.

3.1. **Pre-interpolation based on wavelet transform.** This step corresponds to the part colored red shown in the flowchart of Figure 2. First, using the good multi-resolution capability of wavelet transform [14], the two-dimensional image $f(x, y)$ can be decomposed into four sub-images as shown in the following Equations (1)-(4) after wavelet decomposition at the resolution 2^j.

$$L_j f(x,y) =< f(x,y), \Phi_{j,n}(x)\Phi_{j,m}(y) > \tag{1}$$

$$H_j^1 f(x,y) =< f(x,y), \Phi_{j,n}(x)\Psi_{j,m}(y) > \tag{2}$$

$$H_j^2 f(x,y) =< f(x,y), \Psi_{j,n}(x)\Phi_{j,m}(y) > \tag{3}$$

$$H_j^3 f(x,y) =< f(x,y), \Psi_{j,n}(x)\Psi_{j,m}(y) > \tag{4}$$

In the above equations, Φ, Ψ are wavelet basis function and scale function respectively; $L_j f(x, y)$ is an approximation of the original image, that is, low-frequency information; $H_j^1 f(x, y)$ is the high-frequency information along the horizontal direction;

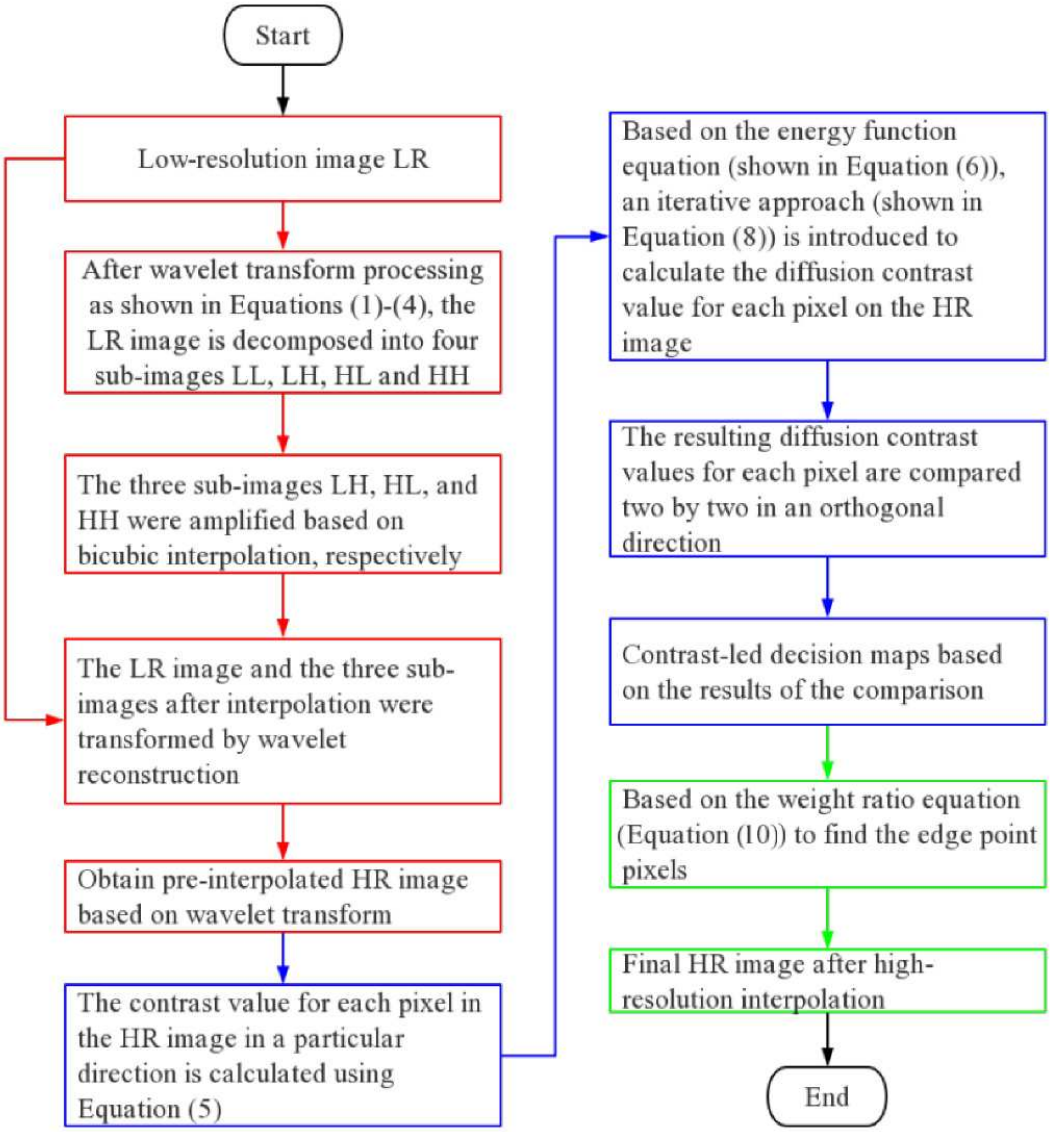

FIGURE 2. (color online) Flowchart of the operation of the algorithm in this study

$H_j^2 f(x,y)$ is the high-frequency information along the vertical direction; $H_j^3 f(x,y)$ is the high-frequency information along the diagonal direction.

Secondly, the three high-frequency sub-images shown in Equations (2)-(4) are interpolated using the bicubic interpolation algorithm. Then, in order to avoid the loss of the low-frequency information that can have some influence on the resultant map, the original low-resolution image LR is used to replace the low-frequency sub-images $L_j f(x,y)$ in the sub-images. Finally, the original low-resolution image LR and the three interpolated sub-images with high-frequency information are transformed by wavelet reconstruction to obtain the final pre-interpolated HR image.

3.2. **Formation of contrast guided decision diagram.** This step corresponds to the part colored blue shown in the flowchart of Figure 2. This step contains the calculation method of edge diffusion in the CGI interpolation algorithm, which calculates the value of diffusion contrast for each pixel point, and uses it to position the edge points, thus retaining the advantage of no loss of edge pixels in the CGI interpolation algorithm. The specific steps of formation of contrast guided decision map are described below.

Let the pixel value of the HR image obtained by pre-interpolation be $I^h(i,j)$. The contrast value of each pixel on the HR image in the θ-direction is calculated by Equation (5).

$$U_\theta^h(i,j) = \left|\nabla_\theta^h I^h(i,j)\right| \tag{5}$$

where ∇_θ^h is the directional derivative. The values of θ in this study are taken as 0°, 45°, 90°, 135° respectively.

The obtained contrast values are diffused by the energy function equation shown below.

$$E(u_\theta) = E_d(u_\theta) + \lambda E_s(u_\theta) \tag{6}$$

where λ is a regular parameter, u_θ is the contrast after diffusion, and $E_d(u_\theta)$ is a data fidelity term, which aims to make the diffused edges maintain their original characteristics. $E_s(u_\theta)$ is a smoothing term, which is used to promote the diffusion of edge pixel points and suppress the diffusion of non-edge pixel points, and its specific algorithm is shown in Equation (7).

$$\begin{aligned} E_d(u_\theta) &= \iint \left(U_\theta^2\left(u_\theta - U_\theta\right)\right) dxdy \\ E_s(u_\theta) &= \iint \left((u_\theta)_x^2 + (u_\theta)_y^2\right) dxdy \end{aligned} \tag{7}$$

At this point, the process of solving for the minimum value of the energy function $E(u_\theta)$ can be transformed into Equation (8).

$$U_\theta^2(u_\theta - U_\theta) - \lambda\nabla^2 u_\theta = 0 \tag{8}$$

where ∇^2 is the Laplace operator, which leads to the equation shown below.

$$\nabla^2 u_\theta = (u_\theta)_{xx} + (u_\theta)_{yy} \tag{9}$$

Thereafter, by introducing an iterative solution, the equation is obtained as shown below.

$$\begin{aligned} u_\theta^{n+1}(i,j) = {} & u_\theta^n(i,j) - U_\theta^2(i,j)\left[u_\theta^n(i,j) - U_\theta(i,j)\right] \\ & - \lambda\left[u_\theta^n(i+1,j) + u_\theta^n(i,j+1) + u_\theta^n(i-1,j)\right. \\ & \left. + u_\theta^n(i,j-1) - 4u_\theta^n(i,j)\right] \end{aligned} \tag{10}$$

From this, the diffusion contrast $u_0^h(i,j)$, $u_{45}^h(i,j)$, $u_{90}^h(i,j)$, $u_{135}^h(i,j)$ of each pixel point on the HR image obtained by pre-interpolation is solved.

The above-mentioned contrast in the four directions is compared two by two in the orthogonal direction. The specific comparison method is shown below.

a. Firstly, comparing the pixel points in the diagonal directions:
   1) If $u_{45}^h(i,j) - u_{135}^h(i,j) > T$, the interpolation direction of this pixel point is 135°;
   2) If $u_{135}^h(i,j) - u_{45}^h(i,j) > T$, the interpolation direction of this pixel point is 45°;
b. After that, comparing the pixels in the horizontal and vertical directions:
   1) If $u_0^h(i,j) - u_{90}^h(i,j) > T$, the interpolation direction of this pixel point is 90°;
   2) If $u_{90}^h(i,j) - u_0^h(i,j) > T$, the interpolation direction of this pixel point is 0°;

where T is the threshold value. In this study, T is taken as the value of 0.021 after the simulation.

3.3. **Finding the edge-point pixels by the equation of weight ratio.** This step corresponds to the part colored green shown in the flowchart of Figure 2. The equation of weight ratio is used to find the pixel values I that were identified as edge points in the previous step. The specific equation is shown below.

$$I = \omega(I_a + I_b) + (0.5 - \omega)(I_c + I_d) \tag{11}$$

where ω is an adjustable parameter. In this study, the value of ω is determined to be 0.575 based on the results of several simulations. And, I_a, I_b, I_c, I_d denote the pixel values of the known pixel points surrounding the pixel point to be calculated. The four known pixel points are selected strictly as indicated by the contrast-guided decision diagram [15].

The image after this step is the final high-resolution HR image after interpolation.

4. **Experimental Results.** In order to objectively evaluate the quality of the images processed by the nearest field interpolation, the bilinear interpolation, the bicubic interpolation, the wavelet transform based interpolation, and the proposed interpolation based on wavelet transform and contrast-guided in this study, the original images are first downsampled in the process of experiment. Then, the downsampled images are interpolated based on the above five algorithms. Finally, the interpolated images are compared with the original images. In this study, the proposed interpolation algorithm based on wavelet transform and contrast-guided is compared with the other four existing interpolation algorithms using stud welding image of anchor chains shown in Figure 3(a) as an example.

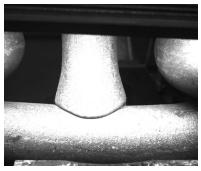

(a) Downsampled image

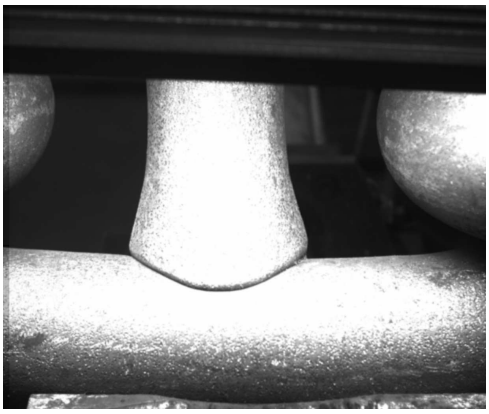

(b) Wavelet transform-based pre-interpolation

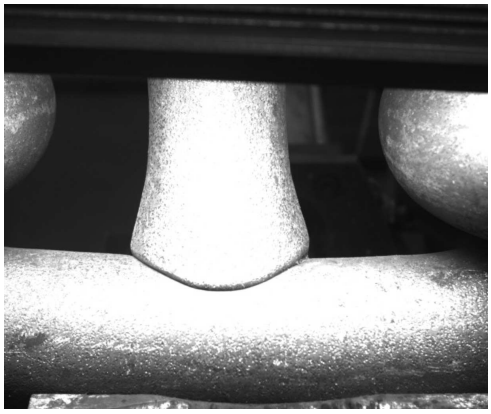

(c) Final image

FIGURE 3. Experimental process

4.1. **Experimental results.** This experiment compares the enhancement effect of the above five interpolation algorithms on the image of the anchor chain transverse weld. Figure 3 shows the experiment results of the interpolation algorithm proposed in this study, and Figure 4 shows the enlarged details of the experiment results of the interpolation algorithm proposed in this study and the experiment results of the bicubic interpolation algorithm.

As shown in Figure 3(a) and Figure 4(a), after the downsampling process, the image loses some pixels, so the jaggedness at the edge of the weld indicated by the arrow is very serious, and the mosaic phenomenon is obvious in the part enclosed by the square frame. After the wavelet transform based pre-interpolation in the interpolation algorithm

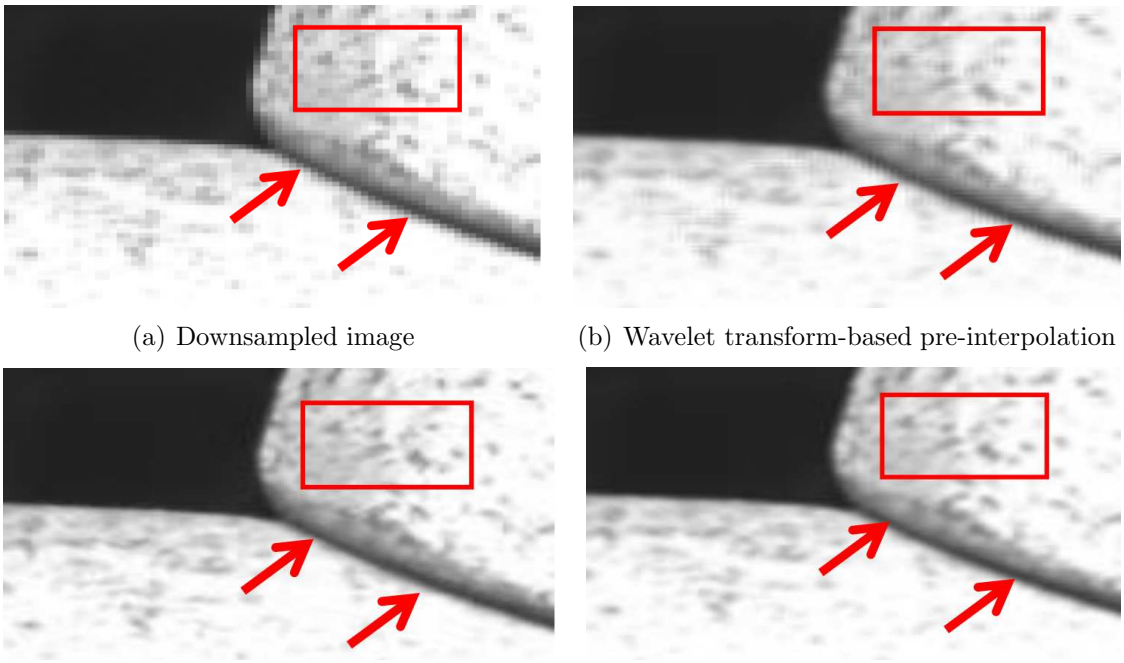

(a) Downsampled image (b) Wavelet transform-based pre-interpolation

(c) Final image (d) Final image of the bicubic interpolation

FIGURE 4. Enlarged detail image

proposed in this study, as shown in Figure 3(b) and Figure 4(b), the sharpness of the weld edge indicated by the arrow is significantly improved compared with Figure 4(a). However, there is still a certain amount of mosaic in the part enclosed within the square frame. After further processing with the contrast guide proposed in this study, as shown in Figure 3(c) and Figure 4(c) with comparison to (a) and (b) of Figure 4, the edge resolution of the resulting final image is further improved, and the mosaic phenomenon in the portion enclosed within the square frame is eliminated. Thus, although the image loses some pixels during the downsampling process, the final images are enhanced to a similar resolution as the input image after the interpolation algorithm proposed in this study.

As a comparison with the algorithms proposed in this study, the same image enhancement process after downsampling was performed for four algorithms which are the nearest field interpolation, the bilinear interpolation, the bicubic interpolation, and the wavelet transform based interpolation, and the results of their standard value measurements are shown in Section 4.2. Among them, the image processed by the bicubic interpolation algorithm is shown in Figure 4(d). According to (c) and (d) of Figure 4, it can be seen that the algorithm of this study has better resolution in the edge part indicated by the arrow, and also has better demosaicing effect in the part surrounded by the square frame.

4.2. **Comparison of standard value measures.** In this study, two aspects of the interpolated images obtained by the five interpolation algorithms are measured. These two aspects of measurement are the comparison of peak signal-to-noise ratio (PSNR) and the comparison of structural similarity (SSIM). The equations for these two measures are shown in Equations (12)-(14).

$$MSE = \frac{\sum_{i=1}^{M} \sum_{j=1}^{N} [HR(i,j) - LR(i,j)]^2}{M * N} \tag{12}$$

$$PSNR = \frac{10 \log_{10} \left(MAX_I^2 \right)}{MSE} \tag{13}$$

$$SSIM = \frac{(2u_x u_y + C_1)(2\sigma_{xy} + C_2)}{(u_x^2 u_y^2 + C_1)(\sigma_x^2 \sigma_y^2 + C_2)} \tag{14}$$

where $M * N$ denotes the size of the image. MSE is the mean square error, which is calculated as the average of the differences in gray values of individual pixel points between the original image and the interpolated image. MAX_I^2 is the square of the maximum pixel value in an image. x, y denote the original image and the interpolated image, respectively. u_x, u_y denote the mean of the two images. σ_x, σ_y denote the standard deviation of the two images. σ_{xy} is the covariance of the two images.

After experimenting with weld images and lena images, Table 1 shows the PSNR between the interpolated image and the original image obtained by the nearest domain interpolation, the bilinear interpolation, the bicubic interpolation, the wavelet transform based interpolation, and the proposed interpolation based on wavelet transform and contrast-guided in this study.

TABLE 1. Comparison of PSNR (in dB) of the interpolated image and the original image by five algorithms

Test images	**Stud welding image**	**Lena**
Nearest field interpolation algorithm	27.8960	31.1610
Bilinear interpolation	27.9285	31.7607
Bicubic interpolation	28.6242	32.5746
Wavelet transform based interpolation algorithm	27.1589	30.9547
The proposed interpolation algorithm in this paper	28.8144	32.4347

Table 2 shows the MSSIN obtained by calculating the SSIM values of the corresponding sub-images of the window and averaging them during the pixel-by-pixel shifting of the 11×11 pixel window over the original image and the interpolated image using the above five algorithms.

TABLE 2. Comparison of MSSIM of the interpolated image and the original image by five algorithms

Test images	**Stud welding image**	**Lena**
Nearest field interpolation algorithm	0.8615	0.9041
Bilinear interpolation	0.8555	0.9116
Bicubic interpolation	0.8777	0.9261
Wavelet transform based interpolation algorithm	0.8483	0.8856
The proposed interpolation algorithm in this paper	0.8794	0.9305

As can be seen from Tables 1 and 2, the PSNR values as well as the MSSIM metrics obtained by the algorithm proposed in this study are higher than those of the other four existing interpolation algorithms.

5. **Conclusion.** In this study, in order to improve the resolution of weld seam images taken by low-resolution cameras using image interpolation techniques for an example of image enhancement of stud welding of anchor chains using robot, an image interpolation enhancement algorithm based on wavelet transform based and contrast-guided was proposed.

First, the wavelet transform based image pre-interpolation was performed for the low-resolution image. Then, a contrast-guided decision map was formed by calculating the diffusion contrast of each pixel of the resulting pre-interpolated image using the edge contrast-guided algorithm. Next, the pixel values of the edge points were more precisely derived based on the resulting decision map and the weight ratio equation of the known pixels around the edge points, which ultimately a high-resolution image of the weld seam was obtained with higher resolution and with the intact image edges. By comparing the nearest field interpolation, the bilinear interpolation, the bicubic interpolation, the wavelet transform based interpolation, and the interpolation based on wavelet transform and contrast-guided proposed in this study for the downsampled weld images, it was shown that the weld image enhancement algorithm proposed in this study has better interpolation effect compared with the other four existing algorithms.

This paper currently performs an algorithmic demonstration of image enhancement of weld images after zooming in four times. Subsequently, the original algorithm can be studied optimally by selecting different wavelet bases for pre-interpolation in order to achieve the purpose of enlarging the image to higher pixels.

REFERENCES

[1] H. Wang, L. Xing, X. Li et al., Analysis of the application status and development of industrial robots, *Mechanical & Electrical Technology*, no.6, pp.115-117, 2018.

[2] Y. Liu, Q. Huang and K. Sato, Differential filtering algorithm for robot welding seam image enhancement, *Journal of Physics Conference Series*, vol.1607, no.1, ID:012045, 2020.

[3] X. You and B. Zhao, Research on laser seam tracking system with automatic calibration function, *Casting Technology*, vol.36, no.7, pp.1829-1832, 2015.

[4] J. Dong, W. Lv, X. Bao et al., Research progress of the PCB surface defect detection method based on machine vision, *Journal of Zhejiang Sci-Tech University (Natural Sciences Edition)*, vol.45, no.3, pp.379-389, 2021.

[5] B. Zhong, Z. Lu and J. Ji, Review on image interpolation techniques, *Journal of Data Acquisition and Processing*, vol.6, no.31, pp.1083-1096, 2016.

[6] H. Chen and X. Guo, Comparative analysis of adaptive and non-adaptive image interpolation algorithms, *Science and Technology Innovation Herald*, vol.17, no.12, pp.128-130, 2020.

[7] K. Zhang, D. Tao, X. Gao et al., Learning multiple linear mappings for efficient single image super-resolution, *IEEE Transactions on Image Processing*, vol.24, no.3, pp.846-861, 2015.

[8] Y. Zhang, X. Zhang, X. Fu et al., Infrared image enhancement algorithm for hot forgings based on wavelet transform and bicubic interpolation, *China Mechanical Engineering*, vol.28, no.17, pp.2095-2099, 2017.

[9] C. Chen, S. Guo, C. Tsai et al., Integer wavelet-based image interpolation in lifting structure for image resolution enhancement, *Applied Mathematics*, vol.9, no.10, pp.1156-1178, 2018.

[10] S.-J. Lee, M.-C. Kang, K.-H. Uhm et al., An edge-guided image interpolation method using Taylor series approximation, *IEEE Transactions on Consumer Electronics*, vol.62, no.2, pp.159-165, 2016.

[11] K. Wang, R. Yang, Y. Yang et al., Design and implementation of image adaptive scaling based on second order Newton interpolation, *Computer Applications and Software*, vol.37, no.9, pp.126-132+138, 2020.

[12] Z. Wei and K. Ma, Contrast-guided image interpolation, *IEEE Transactions on Image Processing*, vol.22, no.11, pp.4271-4285, 2013.

[13] N. Talbi, A. Metatla, N. Ouelaa, R. Younes, L. Fatmi and A. Djebala, Application of the combination of both wavelet multi-resolution analysis and empirical mode analysis to detect induction motor defects, *ICIC Express Letters, Part B: Applications*, vol.10, no.11, pp.1021-1030, 2019.

[14] Y. Zhang, H. Wang, L. Liu et al., A wavelet coefficient interpolation image enhancement based on visual fitting function, *Journal of Terahertz Science and Electronic Information Technology*, vol.17, no.6, pp.1071-1077, 2019.

[15] C. Miao, Y. Xu and Y. Li, Iterative fusion defogging algorithm based on wavelet transform, *Laser & Optoelectronics Progress*, vol.58, no.20, ID:2010018, 2021.

[16] Y. Zhang, X. Yao, F. Bao et al., Adaptive interpolation scheme based on texture features, *Journal of Computer Research and Development*, vol.54, no.9, pp.2077-2091, 2017.

[17] L. Wu, High-resolution images based on directional fusion of gradient, *Computational Visual Media*, vol.2, no.1, pp.31-43, 2016.
[18] Y. Wei and K. Ma, Convolutional edge diffusion for fast contrast-guided image interpolation, *IEEE Signal Processing Letters*, vol.23, no.9, pp.1260-1264, 2016.
[19] C. Dong, C. Loy, K. He and X. Tang, Image super-resolution using deep convolutional networks, *IEEE Transactions on Pattern Analysis and Machine Intelligence*, vol.38, no.2, pp.295-307, 2016.
[20] J. Kim, J. Lee and K. M. Lee, Deeply-recursive convolutional network for image super-resolution, *IEEE Conference on Computer Vision and Pattern Recognition (CVPR)*, pp.1646-1654, 2016.
[21] X. Deng, Y. Zhang, M. Xu et al., Deep coupled feedback network for joint exposure fusion and image super-resolution, *IEEE Transactions on Image Processing*, vol.30, pp.3098-3112, 2021.
[22] Y. Shin, M. Kim, K.-W. Pak and D. Kim, Practical methods of image data preprocessing for enhancing the performance of deep learning based road crack detection, *ICIC Express Letters, Part B: Applications*, vol.11, no.4, pp.373-379, 2020.
[23] L. Yang, W. Wang and X. Wang, Research on edge preserving of single image based on complementary color wavelet transform, *Computer Simulation*, vol.37, no.5, pp.481-485, 2020.
[24] Z. Zhang and J. Lu, Foggy image enhancement based on wavelet transform and improved Retinex, *Computer Applications and Software*, vol.38, no.1, pp.227-231, 2021.
[25] B. Zhong, K. Ma and Z. Lu, Predictor-corrector image interpolation, *Journal of Visual Communication and Image Representation*, vol.61, pp.50-60, 2019.
[26] L. Fang and B. Zhong, Image interpolation with predicted gradients, *Acta Automatica Sinica*, vol.44, no.6, pp.1072-1085, 2018.

Author Biography

Yiying Zhao received her bachelor's degree from Zhejiang Gongshang University (ZJSU), and is now a professional master of the School of Information and Electronic Engineering at ZJSU, with research interests in industrial robotics and machine vision.

Qingjiu Huang received the B.Sc. degree from Huazhong University of Science and Technology, China; the M.Sc. and Ph.D. degrees from Chiba University, Japan. He is currently a Professor at the Control System Laboratory, Graduate School of Engineering, Kogakuin University, Japan. His research interests include the control theory such as robust control, optimal control, adaptive control, and intelligent control; and the kinematics, dynamics, motion control of multi-joint robot arm, multi-legged robot, biped robot, and four-wheel car.